

## Electronic supplementary information

Tailored fabrication of a prospective acousto-optic crystal  $\text{TiTe}_3\text{O}_8$  endowed with high performance

Weiqun Lu, Zeliang Gao,\* Qian Wu, Xiangxin Tian, Youxuan Sun, Yang Liu and Xutang Tao\*

### Contents

**Fig. S1** Temperature dependence of thermal expansion for  $\text{TiTe}_3\text{O}_8$  along the crystallography *a*-axis.

**Fig. S2** Temperature dependence of specific heat for  $\text{TiTe}_3\text{O}_8$ .

**Fig. S3** Thermal diffusivity as a function of temperature for  $\text{TiTe}_3\text{O}_8$  along the crystallography *a*-axis.

**Fig. S4** UV-visible diffuse reflectance spectra data for ground powders of the  $\text{TiTe}_3\text{O}_8$  crystal. The inset shows the relationship between ( $\alpha/S$ ) and  $E$  (eV).

**Table S1** Selected bond lengths (Å) and angles (deg.) in  $\text{TiTe}_3\text{O}_8$ .

**Table S2** Measured values for the refractive indices of  $\text{TiTe}_3\text{O}_8$  at different wavelengths.

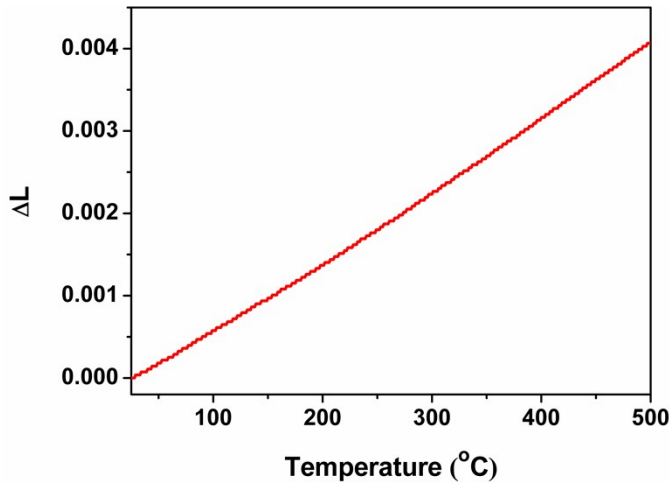


**Fig. S1** Temperature dependence of thermal expansion for  $\text{TiTe}_3\text{O}_8$  along the crystallography  $a$ -axis.

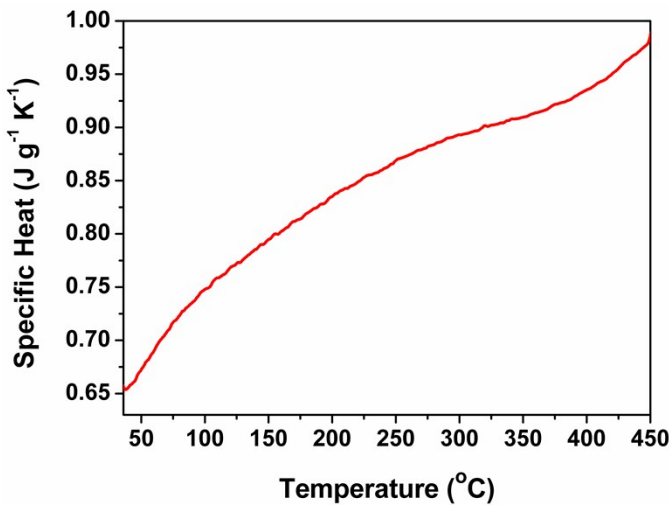


**Fig. S2** Temperature dependence of specific heat for  $\text{TiTe}_3\text{O}_8$ .

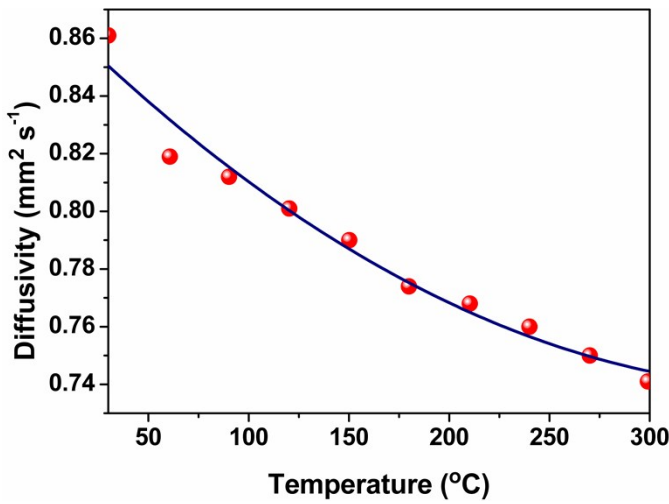


**Fig. S3** Thermal diffusivity as a function of temperature for  $\text{TiTe}_3\text{O}_8$  along the crystallography  $a$ -axis.

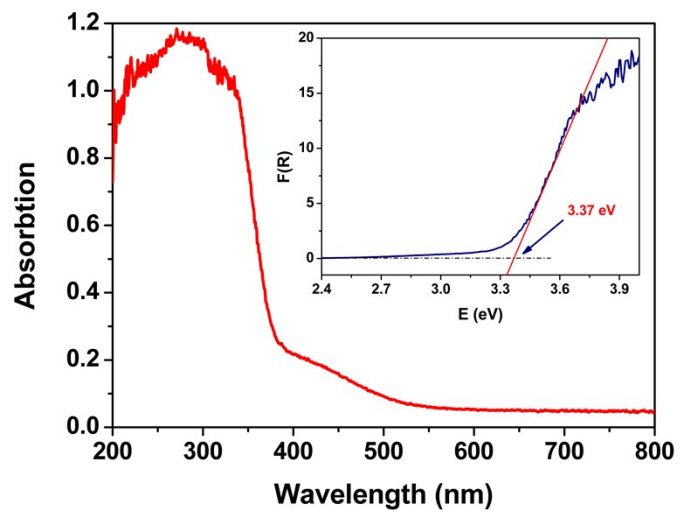


**Fig. S4** UV-visible diffuse reflectance spectra data for ground powders of the  $\text{TiTe}_3\text{O}_8$  crystal. The inset shows the relationship between  $(\alpha/S)$  and  $E$  (eV).

**Table S1** Selected bond lengths (Å) and angles (deg.) in TiTe<sub>3</sub>O<sub>8</sub>.

Te1–O1 <sup>i</sup>	1.884(2)	Ti1–O1 <sup>i</sup>	1.952(2)
Te1–O1 <sup>ii</sup>	1.884(2)	Ti1–O1 <sup>vii</sup>	1.952(2)
Te1–O2	2.1185(7)	Ti1–O1 <sup>viii</sup>	1.952(2)
Te1–O2 <sup>iii</sup>	2.1185(7)	O2–Te1 <sup>ix</sup>	2.1185(7)
Ti1–O1 <sup>iv</sup>	1.952(2)	O2–Te1 <sup>x</sup>	2.1185(7)
Ti1–O1 <sup>v</sup>	1.952(2)	O1–Te1 <sup>xi</sup>	1.884(2)
Ti1–O1 <sup>vi</sup>	1.952(2)	O1–Ti1 <sup>xii</sup>	1.952(2)
O1 <sup>i</sup> –Te1–O1 <sup>ii</sup>	101.79(16)	O1 <sup>v</sup> –Ti1–O1 <sup>vii</sup>	91.81(9)
O1 <sup>i</sup> –Te1–O2	86.02(13)	O1 <sup>vi</sup> –Ti1–O1 <sup>vii</sup>	88.19(9)
O1 <sup>ii</sup> –Te1–O2	79.99(8)	O1 <sup>i</sup> –Ti1–O1 <sup>vi</sup>	91.81(9)
O1 <sup>i</sup> –Te1–O2 <sup>iii</sup>	79.99(8)	O1 <sup>iv</sup> –Ti1–O1 <sup>viii</sup>	91.81(9)
O1 <sup>ii</sup> –Te1–O2 <sup>iii</sup>	86.02(13)	O1 <sup>v</sup> –Ti1–O1 <sup>viii</sup>	88.19(9)
O2–Te1–O2 <sup>iii</sup>	157.76(13)	O1 <sup>vi</sup> –Ti1–O1 <sup>viii</sup>	91.81(9)
O1 <sup>iv</sup> –Ti1–O1 <sup>v</sup>	180.0(2)	O1 <sup>i</sup> –Ti1–O1 <sup>viii</sup>	88.19(9)
O1 <sup>iv</sup> –Ti1–O1 <sup>vi</sup>	91.81(9)	O1 <sup>vii</sup> –Ti1–O1 <sup>viii</sup>	180.0(2)
O1 <sup>v</sup> –Ti1–O1 <sup>vi</sup>	88.19(9)	Te1 <sup>ix</sup> –O2–Te1	116.86(6)
O1 <sup>iv</sup> –Ti1–O1 <sup>i</sup>	88.19(9)	Te1 <sup>ix</sup> –O2–Te1 <sup>x</sup>	116.86(6)
O1 <sup>v</sup> –Ti1–O1 <sup>i</sup>	91.81(9)	Te1–O2–Te1 <sup>x</sup>	116.86(6)
O1 <sup>vi</sup> –Ti1–O1 <sup>i</sup>	180.0(2)	Te1 <sup>xi</sup> –O1–Ti1 <sup>xii</sup>	138.28(13)
O1 <sup>iv</sup> –Ti1–O1 <sup>vii</sup>	88.19(9)		

Symmetry codes: (i)  $y-1/2, -z+1/2, -x$ ; (ii)  $-y+1/2, z, -x$ ; (iii)  $-x, -y+1/2, z$ ; (iv)  $x, -y+1/2, z-1/2$ ; (v)  $-x, y-1/2, -z+1/2$ ; (vi)  $-y+1/2, z-1/2, x$ ; (vii)  $-z+1/2, -x, y-1/2$ ; (viii)  $z-1/2, x, -y+1/2$ ; (ix)  $y, z, x$ ; (x)  $z, x, y$ ; (xi)  $-z, -x+1/2, y$ ; (xii)  $-x, y+1/2, -z+1/2$ .

**Table S2** Measured values for the refractive indices of TiTe<sub>3</sub>O<sub>8</sub> at different wavelengths.

$\lambda$ (nm)	$n$
546.075	2.382467
587.562	2.359446
643.847	2.336531
706.519	2.318121
852.11	2.291467
1013.98	2.274489
1529.58	2.252335
2325.42	2.231389